Plasma sheet formation during long period of northward IMF

Wenhui Li,[1] Joachim Raeder,[1] John Dorelli,[1] Marit Øieroset,[2] and Tai D. Phan[2]

Received 15 September 2004; revised 31 January 2005; accepted 18 February 2005; published 28 April 2005.

[1] We have studied the entry paths of solar wind plasma into the magnetosphere during an extended period of northward IMF using an OpenGGCM MHD simulation of the cold dense plasma sheet (CDPS) event observed on October 23, 2003 by the Cluster spacecraft. We find that high-latitude reconnection occurs tailward of both cusps between the IMF and geomagnetic field. The newly created closed magnetic flux tubes capture magnetosheath plasma, and subsequently sink and shrink into the magnetosphere, while convecting tailward. The plasma that enters near the reconnection site is driven sunward and toward the low latitude region initially; it then drifts to the flanks. The captured plasma is characterized by small flow velocity, and it is moderately heated in the reconnection region. In the present case study we find the cold plasma enters the plasma sheet in the near Earth tail where it is observed by Cluster.
Citation: Li, W., J. Raeder, J. Dorelli, M. Øieroset, and T. D. Phan (2005), Plasma sheet formation during long period of northward IMF, *Geophys. Res. Lett.*, *32*, L12S08, doi:10.1029/2004GL021524.

1. Introduction

[2] It is well known that the solar wind plasma can enter into the plasma sheet through reconnection processes first at the dayside subsolar merging site and then in the distant magnetotail, when the IMF is southward [*Dungey*, 1961; *Cowley*, 1980; *Rosenbauer et al.*, 1975; *Sckopke et al.*, 1981]. The first reconnection process captures the solar wind plasma which then flows tailward into the mantle/lobe. The second reconnection drives the plasma from the mantle/lobe toward the Earth. As a consequence of the reconnection process the plasma sheet is most of the time found to be consisting of hot (1–10 keV) and tenuous plasma. It becomes denser and hotter for increasing geomagnetic activity [*Borovsky et al.*, 1998; *Wing and Newell*, 1998].

[3] When the IMF is northward, there is no or little dayside reconnection. The plasma sheet density should therefore decrease. However, the plasma sheet often becomes denser and colder under quiet geomagnetic conditions. At times, a very cold and dense plasma sheet is observed [e.g., *Fairfield et al.*, 1981; *Baumjohann et al.*, 1989; *Lennartsson*, 1992; *Fujimoto et al.*, 1996, 1998; *Terasawa et al.*, 1997]. The ionosphere is an unlikely source of this plasma since (1) the ionospheric outflow has been found to be strongest during active times and for southward IMF [*Yau et al.*, 1985; *Øieroset et al.*, 1999], and (2) the CDPS is generally absent of a cold O^+ component [e.g., *Rème et al.*, 2001]. Therefore, the plasma entering the plasma sheet when the IMF is northward is believed to be primarily of solar wind origin.

[4] Most of the CDPS observations are made near the Earth in the tail ($X_{GSE} > -30\ R_E$). The CDPS is often observed after a period when the IMF had been northward, on average, for several hours. This plasma is characterized by higher density ($\sim$1 cm^{-3}), lower temperature (<1 keV), and small flow velocity. It is found to be on closed field lines [*Fujimoto et al.*, 1998]. *Terasawa et al.* [1997] found it could be a temporal state of the plasma sheet. Many observations show that it is located much more often near the flanks [e.g., *Fujimoto et al.*, 1996, 1998; *Phan et al.*, 1998; *Fuselier et al.*, 1999; *Øieroset et al.*, 2002] than at the center of the plasma sheet.

[5] The following mechanisms of solar wind plasma entry have been proposed to account for the CDPS: (1) a diffusive process (Kelvin-Helmholtz) along the tail flank [*Terasawa et al.*, 1997; *Fairfield et al.*, 2000]; (2) entry through high-latitude reconnection between the lobe field and the northward IMF at both hemispheres [*Song and Russell*, 1992; *Song et al.*, 1999; *Raeder et al.*, 1995, 1997]. However, neither of these studies show in sufficient detail how the plasma enters into the plasma sheet and what its expected properties are.

[6] In the present study, we investigate the solar wind plasma entry mechanism by analyzing global simulation results for a real CDPS event observed by Cluster which is presented in the accompanying paper by *Øieroset et al.* [2005]. The companion paper discusses in detail the Cluster and related solar wind and IMF observations. That paper also presents a comparison of the data with time series taken from our simulation. At least during the first half day of the event the simulation results match the Cluster data in the tail remarkably well. We take this as an indication that the simulation captures the correct physical process that leads to the CDPS formation, although we can not exclude other processes, for example diffusion, that are not included in our model. Based on these results we take the next step in this paper and investigate the CDPS formation process in more detail.

2. Simulation

[7] Cluster observed an extended period of cold dense plasma from 2128 UT on October 22 to 0343 UT on October 24, 2003 [*Øieroset et al.*, 2005]. During the same time period, ACE observed steady strong Northward IMF. We ran a simulation for this event with the OpenGGCM MHD model [*Raeder*, 2003], using ACE solar wind and IMF data as input. The simulated time period is from 1500 UT on October 22 to 0300 UT on October 24, 2003. Full 3D data dumps of the simulation results are output

[1]Space Science Center, University of New Hampshire, Durham, New Hampshire, USA.
[2]Space Sciences Laboratory, University of California, Berkeley, California, USA.

0094-8276/05/2004GL021524$05.00

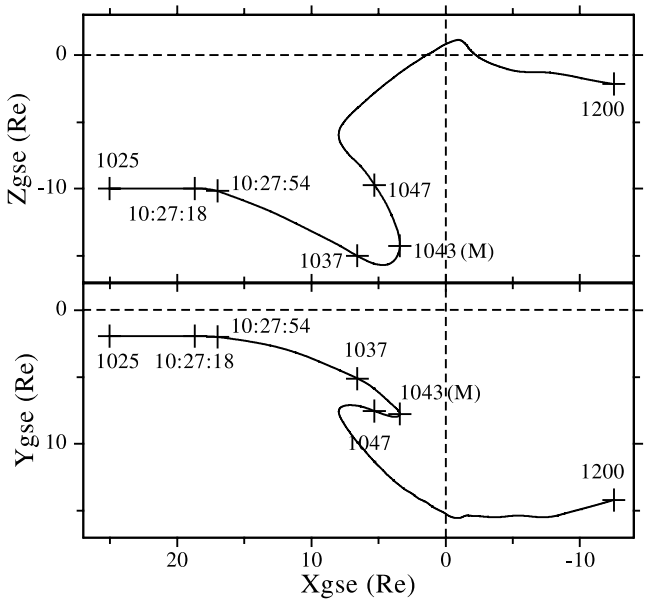

Figure 1. One typical plasma flow path that passes near the Cluster position at 1200 UT on October 23, 2003. The time marks between 1025 and 1200 are correspond to the vertical lines and point M in Figure 2.

every 300 seconds. The grid dimensions are $(-601, 25) \times (-45, 45) \times (-45, 45)$ R_E in GSE coordinates, and its resolution is 0.3 R_E in subsolar region and 0.5–1 R_E in the flanks. The primary output parameters are flow velocity components, magnetic field components, plasma density and plasma pressure.

3. Entry Path

[8] Based on this simulation output data, we trace observed plasma parcels backward in time. We select a few locations around the position where the Cluster observed the cold dense plasma as the seed points. Then we trace backward the plasma flow using the flow velocity field data from the simulation, i.e.,

$$\frac{d\vec{X}(t)}{dt} = -\vec{V}\left(\vec{X}(t), t\right). \quad (1)$$

[9] Because the velocity data from the simulation are gridded in space and time, we use linear interpolation in both space and time to compute the right hand side of equation (1).

[10] Figure 1 shows a typical tracing result for a seed point near the Cluster location $(-12.5, 14.0, -2.1)$ R_E in GSE coordinates at 1200 UT on October 23. This plasma parcel starts at 1025 UT in the solar wind. It then moves across the bow shock from 10:27:18 UT to 10:27:54 UT, and traverses the magnetosheath until 1037 UT. At this time, it enters the magnetosphere and is captured on a closed field line. It is subsequently driven northward and sunward in the reconnection zone until 1047 UT. This plasma parcel continues to move northward and sunward for a while, then turns tailward and toward the dusk side to the flank area. The same time marks are used in Figure 2, which shows the variation of plasma and field parameters along this path of the parcel. At 1043 UT, the parcel is closest to the magnetic null point. This is indicated by the point M shown in Figure 2. The typical transport time to the Cluster location at $(-12.5, 14.0, -2.1)$ R_E is about 1.5 hours.

[11] Figure 2 shows several MHD parameters along this path. The panels from the top are plasma temperature, plasma density, magnetic field, flow velocity and its Z-component. Corresponding to the abrupt changes of the parameter values, the first and second vertical lines define the time at which the plasma moves across the bow shock boundaries. The third vertical line approximately defines the time at which the plasma parcel exits the magnetosheath and enters the magnetosphere. It is estimated according to the acceleration in Z direction and the temperature enhancement at this time. This time is also in agreement with the time associated with the first closed field line shown in Figure 3 (see discussion below). The dotted fourth vertical line indicates the time at which the northward velocity reaches its maximum. The third and fourth vertical lines approximately define the time period during which the parcel is influenced by the cusp reconnection. The minimum magnitude of the magnetic field indicated by the point M suggests that the plasma is passing near the magnetic nulls associated with cusp reconnection. The velocity panels show that the flow is continuously slowing down in the magnetosheath and is further decelerated when it goes toward the reconnection site. It is likely that there is an outflow force from the reconnection site to slow down the plasma, reflect it back and push it northward for some time

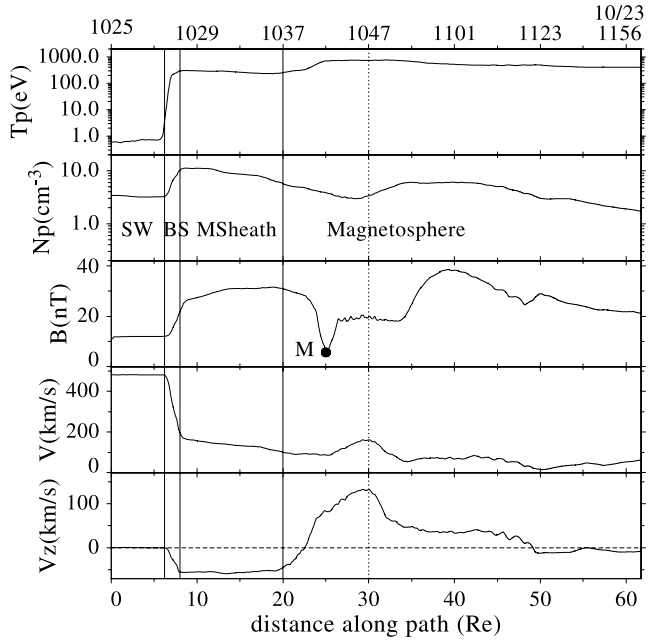

Figure 2. MHD parameters along the path shown in Figure 1. The top axis is labeled with the corresponding time. The four vertical lines are corresponding to time 10:27:18, 10:27:54, 10:37:00, and 10:47:00, respectively. Point M is at time 10:43:00 UT. SW, BS and MSheath denote the regions and stand for solar wind, bow shock and magnetosheath, respectively.

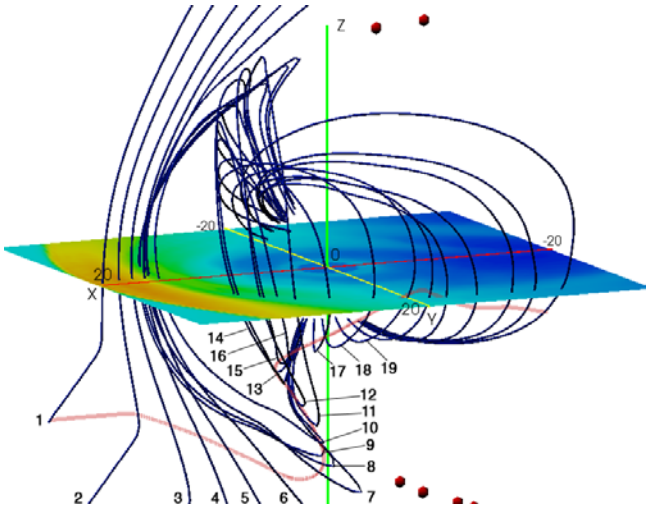

Figure 3. Three dimensional visualization of the solar wind plasma entry process. The equatorial plane is a color map of the plasma density. The pink curve is the path shown in Figure 1. The dark blue lines are this path's frozen-in magnetic field lines. The red dots are the magnetic nulls. The red, yellow, and green axes are GSE X, Y, and Z axes, respectively. The first 19 field lines are labeled with numbers sequentially in time.

until it is out of the influence of the reconnection region. After entering the magnetosphere, the flow is very slow most of the time except for the small increase near the reconnection site. The density is greater than 1 cm^{-3} throughout, which is substantially larger than the typical plasma sheet density, but is smaller than the magnetosheath density. The temperature panel shows that the plasma is heated by a factor of 3 when it travels from the magnetosheath into the magnetosphere.

[12] Figure 3 shows a 3D visualization of the path in Figure 1, the plasma's frozen-in magnetic field lines, the equatorial plane color coded with plasma density at 1030 UT, and the magnetic nulls at this time. This figure displays how the magnetosheath plasma enters the magnetosphere. The magnetosheath on the equatorial plane appears as the yellow ribbon on the color map. The 7th to 10th magnetic field lines look like they result from reconnection between lobe field lines and magnetosheath field lines, especially the 10th field line which is very close to the magnetic null at about $(-0.6, 12.0, -15.1)$ R_E. These field lines clearly indicate that there is magnetic tension at the sharply kinked section parallel to magnetopause that slows down the plasma, even turns it slightly sunward, and pushes it northward. This tension force also causes a drift with northward velocity component for ions on this kinked field line section. The 7th to 19th field lines show how the newly created closed flux tube sinks into the magnetosphere and sweeps around the flank to the tail.

4. Discussion

[13] Long duration events of nearly pure northward IMF are rare. The October 23 event therefore provides an excellent opportunity to test and extend our models.

[14] Capturing of magnetosheath plasma by high-latitude reconnection has been first proposed by *Song and Russell* [2002] to explain the formation of LLBL under northward IMF conditions. In this model, IMF flux tubes pass through the subsolar point where the solar wind is almost stagnant. Reconnection then occurs for such flux tubes tailward of the cusps in both hemispheres. The model also describes the process of sinking and reorientation of the newly created closed flux tubes into the magnetosphere. Figure 3 shows a very similar process. The to-be-reconnected IMF flux tube first drapes over the dayside magnetopause. Once reconnected, it sinks and contracts into the magnetosphere. Subsequently it sweeps around the flank, and is convected tailward at the same time. During this process, the plasma in the southern (northern) part of the flux tube is pulled northward (southward) and sunward. *Song and Russell* [2002] did not discuss the sinking process in detail. Figure 3 indicates that magnetic tension plays a dominant role because the flux tubes first straighten out just after reconnection occurs.

[15] The magnetosheath plasma near the subsolar region is cold, dense and almost stagnant. As the plasma is captured and transported to the tail, it is moderately heated near the reconnection site, and the temperature is just below 1 keV as shown in Figure 2. The density in the captured flux tubes is ultimately lower than the magnetosheath density. A possible reason is that the captured plasma expands in the parallel direction toward the Earth along the flux tube, and in perpendicular direction to enlarge its volume. In spite of this, the density is still greater than 1 cm^{-3} throughout. After entering the magnetosphere, the plasma flow speed stays small except that there is a small bump near the reconnection site as shown in the velocity panel of Figure 2. Therefore the CDPS is characteristic of cold, dense and almost stagnant plasma. The values of temperature, density and low flow speed for the captured plasma are in good agreement with CDPS observations in this event [*Øieroset et al.*, 2005].

[16] Our simulation shows that cusp reconnection and the associated capture of magnetosheath plasma is sufficient to produce a cold dense plasma sheet. Kelvin-Helmholtz mediated diffusion has also been suggested as a possible entry process [*Fairfield et al.*, 2000]. In our simulation we do not observe any K-H waves at the dayside or flank magnetopause. This could be either due to the fact that the K-H waves are stable during the prevailing conditions or because the simulation does not resolve K-H waves sufficiently. In future studies, with higher numerical resolution, we will hopefully be able to answer this question.

[17] **Acknowledgments.** We would like to thank the ACE plasma and magnetometer teams for providing their data. We thank Tom Fogal for his assistance in producing Figure 3. Computations were performed at the National Center for Supercomputer Applications (NCSA) and at the San Diego Supercomputer Center (SDSC). The work at UNH was supported by NSF grants ATM 0353211 and ATM 0441046.

References

Baumjohann, W., G. Paschmann, and C. A. Cattell (1989), Average plasma properties in the central plasma sheet, *J. Geophys. Res.*, *94*, 6597.

Borovsky, J. E., M. F. Thomsen, and R. C. Elphic (1998), The driving of the plasma sheet by the solar wind, *J. Geophys. Res.*, *103*, 17,617.

Cowley, S. W. H. (1980), Plasma poulations in a simple open model magnetosphere, *Space Sci. Rev.*, *26*, 217.

Dungey, J. W. (1961), Interplanetary magnetic field and the auroral zones, *Phys. Rev. Lett.*, *6*, 47.

Fairfield, D. H., R. P. Lepping, E. W. Hones, S. J. Bame, and J. R. Asbridge (1981), Simultaneous measurements of magnetotail dynamics by IMP spacecraft, *J. Geophys. Res.*, *86*, 1396.

Fairfield, D. H., A. Otto, T. Mukai, S. Kokubun, R. P. Lepping, J. T. Steinberg, A. J. Lazarus, and T. Yamamoto (2000), Geotail observations of the Kelvin-Helmholtz instability at the equatorial magnetotail boundary for parallel northward fields, *J. Geophys. Res.*, *105*, 21,159.

Fujimoto, M., A. Nishida, T. Mukai, Y. Saito, T. Yamamoto, and S. Kokubun (1996), Plasma entry from the flanks of the near-Earth magnetotail: Geotail observations in the dawnside LLBL and the plasma sheet, *J. Geomagn. Geoelectr.*, *48*, 711.

Fujimoto, M., T. Terasawa, T. Mukai, Y. Saito, T. Yamamoto, and S. Kokubun (1998), Plasma entry from the flanks of the near-Earth magnetotail: Geotail observations, *J. Geophys. Res.*, *103*, 4391.

Fuselier, S. A., R. C. Elphic, and J. T. Gosling (1999), Composition measurements in the dusk flank magnetosphere, *J. Geophys. Res.*, *104*, 4515.

Lennartsson, W. (1992), A scenario for solar wind penetration of Earth's magnetic tail based on ion composition data from the ISEE 1 spacecraft, *J. Geophys. Res.*, *97*, 19,221.

Øieroset, M., M. Yamauchi, L. Liszka, and B. Hultqvist (1999), Energetic ion outflow from the dayside ionosphere: Categorization, classification, and statistical study, *J. Geophys. Res.*, *104*, 24,915.

Øieroset, M., et al. (2002), Spatial and temporal variations of the cold dense plasma sheet: Evidence for a low-latitude boundary layer source? in *Earth's Low-Latitude Boundary Layer*, *Geophys. Monogr. Ser.*, vol. 133, edited by P. T. Newell and T. G. Onsager, p. 253, AGU, Washington, D. C.

Øieroset, M., J. Raeder, T. D. Phan, S. Wing, J. P. McFadden, W. Li, M. Fujimoto, H. Rème, and A. Balogh (2005), Global cooling and densification of the plasma sheet during an extended period of purely northward IMF on October 22–24, 2003, *Geophys. Res. Lett.*, *32*, L12S07, doi:10.1029/2004GL021523.

Phan, T. D., G. Paschmann, A. Raj, V. Angelopoulos, D. Larson, and R. P. Lin (1998), Wind observations of the halo/cold plasma sheet, in *Substorms-4*, edited by S. Kokubun and Y. Kamide, Terra Sci., Tokyo.

Raeder, J. (2003), Global geospace modeling: Tutorial and review, in *Space Plasma Simulation*, edited by J. Büchner, C. T. Dum, and M. Scholer, Springer, New York.

Raeder, J., R. J. Walker, and M. Ashour-Abdalla (1995), The structure of the distant geomagnetic tail during long periods of northward IMF, *Geophys. Res. Lett.*, *22*, 349.

Raeder, J., et al. (1997), Boundary layer formation in the magnetotail: Geotail observations and comparisons with a global MHD model, *Geophys. Res. Lett.*, *24*, 951.

Rème, H., C. Aoustin, M. Bosqued, I. Dandouras, and the CIS-Team (2001), First multispacecraft ion measurements in and near the Earth's magnetosphere with the identical Cluster Ion Spectrometry (CIS) Experiment, *Ann. Geophys.*, *19*, 1303.

Rosenbauer, H., H. Grunwaldt, M. D. Montgomery, G. Paschmann, and N. Sckopke (1975), Heos 2 plasma observations in the distant polar magnetosphere: The plasma mantle, *J. Geophys. Res.*, *80*, 2723.

Sckopke, N., G. Paschmann, G. Haerendel, B. U. O. Sonnerup, S. J. Bame, T. G. Forbes, E. W. Hones, and C. T. Russell (1981), Structure of the low-latitude boundary layer, *J. Geophys. Res.*, *86*, 2099.

Song, P., and C. T. Russell (1992), Model of the formation of the low-latitude boundary layer for strongly northward interplanetary magnetic field, *J. Geophys. Res.*, *97*, 1411.

Song, P., D. L. DeZeeuw, T. I. Gombosi, C. P. T. Groth, and K. G. Powell (1999), A numerical study of solar wind-magnetosphere interaction for northward interplanetary magnetic field, *J. Geophys. Res.*, *104*, 28,361.

Terasawa, T., et al. (1997), Solar wind control of density and temperature in the near-earh plasma sheet: Wind/Geotail collaboration, *Geophys. Res. Lett.*, *24*, 935.

Wing, S., and P. T. Newell (1998), Central plasma sheet ion properties as inferred from ionosphere observations, *J. Geophys. Res.*, *103*, 6785.

Yau, A. W., E. G. Shelley, W. K. Peterson, and L. Lenchyshyn (1985), Energetic auroral and polar ion outflow at DE 1 altitudes: Magnitude, composition, magnetic activity dependence, and long-term variations, *J. Geophys. Res.*, *90*, 8417.

J. Dorelli, W. Li, and J. Raeder, Space Science Center, University of New Hampshire, Morse Hall, Durham, NH 03824, USA. (john.dorelli@unh.edu; wenhuil@cisunix.unh.edu; j.raeder@unh.edu)

M. Øieroset and T. D. Phan, Space Sciences Laboratory, University of California, Berkeley, CA 94720, USA. (oieroset@ssl.berkeley.edu; phan@ssl.berkeley.edu)